

# Mechanical and Electrical Characterization of Nanocomposites Liquid-Solid Conductive Ink on Polyethylene Terephthalate (PET) Substrate

Norhisham Ismail<sup>1</sup>, Mohd Azli Salim<sup>1\*</sup> Adzni Md Saad<sup>1</sup>, Nor Azmmi Masripan<sup>1</sup> and Ghazali Omar<sup>1</sup>

<sup>1</sup>Universiti Teknikal Malaysia Melaka, Hang Tuah Jaya, Durian Tunggal, Melaka, Malaysia

## ABSTRACT

*With drastic development of wearable electronics have urged the studies on the conductive ink and flexible substrate. Wearable electronics consist of nanocomposites liquid-solid conductive ink and flexible substrate such as polyethylene terephthalate (PET). They were produced by using stencil printing method. This paper presents the mechanical and electrical characteristics of conductive ink with unloaded condition. The conductive ink was printed with four patterns, which were straight, curve, square and zig-zag patterns. Then, all four patterns were tested for their surface morphology, surface roughness, sheet resistivity and bulk resistivity. Surface morphology showed that conductive ink with 3 mm width had less granular particle formed than conductive ink with 1 mm width. Surface roughness of conductive ink with 3 mm width was smoother compared to 2 mm width and 1 mm width. Sheet resistivity and bulk resistivity results indicated that resistivity of all four patterns decreased with the increase of the conductive ink width. From the result, it showed that conductive ink with straight pattern has the best performance. Meanwhile, individual result for each pattern had its own function inside the circuit track.*

**Keywords:** liquid-solid conductive ink, mechanical and electrical characteristic, polyethylene terephthalate, stencil printing method, wearable electronics.

## 1. INTRODUCTION

Nanocomposites liquid-solid conductive ink had become the focus and mostly researched material nowadays because it can update and enhance the properties and multi-functionalities of existing material. With the combination of flexible substrate, this advanced material technology also benefits electronic industry like electronic packaging, flexible display, wearable electronic, clothing, and sensor [1][2] which most of them need integration on surface, micro size and thin thickness devices. These flexible and wearable devices use substrate that allows roll-up, roll-to-roll, stretchable, twist and bend behavior. By replacing the thick and hard substrate, the advantages of flexibility, lightweight, and toughness can be achieved with flexible substrate [3][4]. Polyethylene terephthalate (PET) is one of the flexible material that suitable to be used as a substrate. PET is a strong, stiff and belongs to the group in the polyester family of polymers [5]. They are highly resistance to deformation which is hard to wrinkle. PET is usually used in durable-press blends with other fibers, which provides the fiber or fabric to recover from wrinkling. In other case, with slightly higher molecular weight, high-strength plastic can be produced by all the other thermoplastic methods.

Liquid-solid conductive ink is material that converts insulative polymers into conductive material. There are several types of conductive filler that have been developed such as metal-based inks, carbon complexes, and conductive polymers [6] Insulative polymers usually can be grouped into thermosetting resins and thermoplastic resins, where they were formed in three-dimensional, which won't melt again even they were heated repeatedly. Whereas, the later are chain polymers, which can melt again after heated even after molded. This prove that thermoplastic resins can be used to thermally bond the nanofiller and insulative polymer. Direct bonding [7] can be used to bond nanofiller and insulative polymer together using chemical and thermal process method. Chemical bonding method modifies the bonding surfaces into contact

\*Corresponding author. Email: azli@utem.edu.my

chemically and then bonding them together. For thermal bonding method, it uses thermal to soften and welds the contact surfaces and then cooling it after contact surfaces are welded.

Insulative polymer were added with conductive nanofiller until the conductive network was formed inside the polymer matrix. In other case, with randomly dispersed and high loading of conductive nanofiller may not form a network between insulative polymers and conductive nanofiller, which causing the material to become relatively weak brittle structure [3], [8]. Also, there are quite a challenge to control and manipulate the nanoparticles in order to produce remarkable and effective electric properties [9].

However, nanocomposites show excellent properties, where they have excellent high surface to volume ratio of the nanofiller or high aspect ratio, exceptional strength and toughness, also electrical and thermal conductivity, combine with their low cost and easy of processability[6]. Electrical conductivity that can fulfill the needs of the application and mechanical properties of the ink were important [10]. So the ink must be defect free such as pore, delamination, porosity and crack, and had good adhesion between substrate and ink [8], [10].

In this paper, four patterns of conductive ink were printed on PET substrate with three different track width such as 1 mm, 2 mm, and 3 mm. These patterns were commonly used inside circuit track. After that, the samples were tested with several tests such as surface morphology, surface roughness, sheet resistivity, and bulk resistivity to characterize their mechanical and electrical characteristics under static condition or unloaded condition. From the test, the characteristic for each pattern and effect of the parameter can be observed and analyzed.

## 2. EXPERIMENTAL ARRANGEMENT

Surface morphology, surface roughness, bulk resistance, and sheet resistance of prepared samples were measured with respective devices.

### 2.1 Sample Preparation

Stencil printing method was used as printing method to print the samples on polyethylene terephthalate (PET) substrate. This method required the conductive ink to be direct-write on top of the stencil to acquire the desired shape as figure 1. Carbon based liquid-solid ink was used as the material and printed into four different test patterns as shown in Figure 1. These test patterns were chosen by considering of many shapes and turns inside an electronic circuit track.

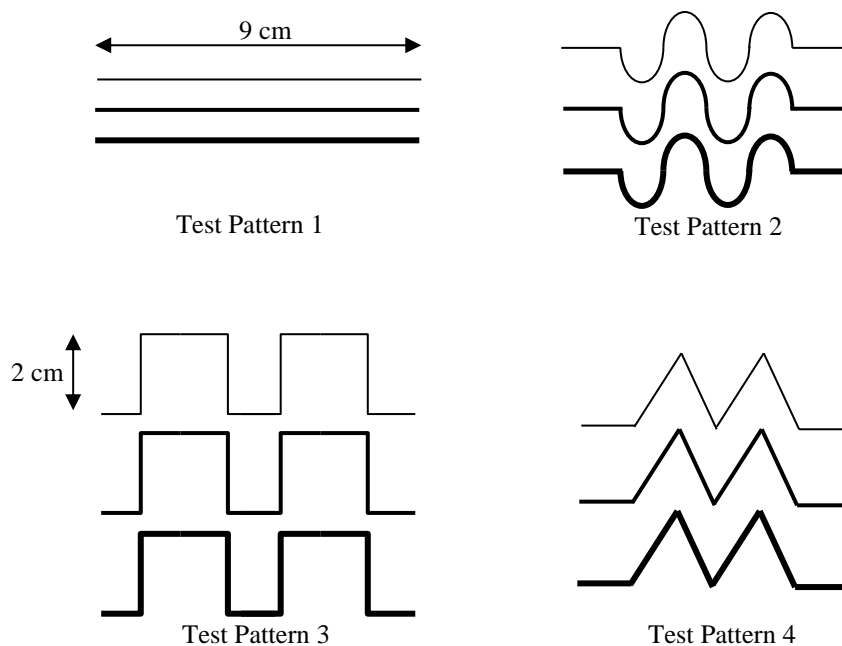


Figure 1: Conductive ink's test patterns

In this project, test pattern 1 was straight line pattern, test pattern 2 was curve pattern, test pattern 3 was square pattern, and test pattern 4 was zig-zag pattern. They were directly printed with stencil jig. All the patterns were designed with 9 cm x 2 cm of length, and width, and 1 mm of thickness as in Figure 1. Each test pattern was printed with track width of 1 mm, 2 mm, and 3 mm, and cured at room temperature for at least 15 minutes. PET was used as ink substrate due to its flexibility, good chemical resistance to alkalis and good mechanical properties such as stiffness, absorb very small amount of water, and strong with less cost and thin thickness [11]. Also, the crystallinity of the PET varies from amorphous to fairly high crystalline.

Four test patterns that had been printed will undergo a few characterization tests to characterize their mechanical and electrical characteristics such as surface morphology, surface roughness, bulk resistivity, and sheet resistivity. In order to determine the testing point and to ensure consistency of the data, all the samples were marked at three points like figure 2 and all the tests was done on the marked point.

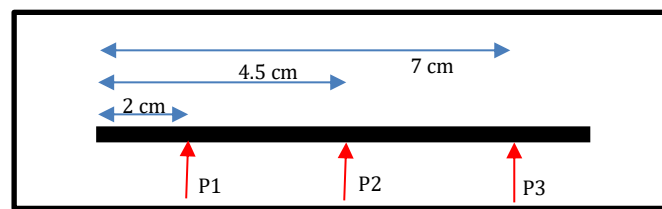


Figure 2: Measurement point on the sample

## 2.2 Measurements

Sample's mechanical characteristic such as surface morphology and surface roughness, and electrical characteristic such as bulk resistivity and sheet resistivity were observed and measured with 3D non-contact profilometer, multimeter and four-point probe. All these tests were done on the samples with unloaded condition.

### 2.2.1 Surface Morphology and Surface Roughness

Surface morphology and surface roughness were measured with 3D non-contact profilometer, which has interference microscopes with wavelength of light as the ruler to measure height variations like surface roughness with high precision. It can be used for single point, a line, and three dimensional scan. This profilometer measured the optical path differences of the samples, which were the height variances on the samples surface.

In this experiment, sample was put on the profilometer platform and pinned with tape to keep it from shaking and remain stationary and flat during 3D scanning process and image taking process. The marked point as in Figure 2 was focused with fine focus with 20x magnification objective lens. 3D non-contact profilometer scanned and measured height, which was Z-axis over an area of X and Y. Lateral dimensions, which the lowest height of focus area was set as start measuring point and the highest height of focus area as end of measuring point. With the help of software, which was connected live with the profilometer, it showed surface condition of focus area including peaks, valleys, steps, voids, and flat surface and all the images were collected into Table 1.

For surface roughness or arithmetic average height, Ra was measured by continuing the surface morphology process with 3D non-contact profilometer. After the focus area was scanned, the 3D image was transferred and projected inside 3D profile section. The analysis process was done in 3D profile as in Figure 3, where 3D roughness profile calculates an area of the scanned surface instead of a single line. Generally, inside the software, the 3D profile was divide



number of sections over one sampling length,  $l$ , from this, the parameters of several 2D roughness profiles that projecting a number of consequents profiles from surface was calculated for each sections.

When 3D profile was scanned, consequent profiles were projected with the direction of X-axis and magnification at Y-axis. There was mean line between peaks and valleys of the profile. In 2D roughness profile, area of peaks and valleys from mean line over each section,  $y_i$ , were taken. Then, the roughness was obtained when average of parameter for each section was taken. Therefore, mathematical definition and digital implementation were shown as below;

$$R_a = \frac{1}{l} \int_0^l |y(x)| dx$$

$$R_a = \sum_{i=1}^n |y_i|$$

Three lines or 2D profile across the focus area were set and measured to get their average surface roughness,  $R_a$ .  $R_a$  used a set of individual measurements of peaks and valleys from each lines into average value. Each of the data of  $R_a$  was recorded into table, which consisted of three lines at every point of the samples and also their averages.

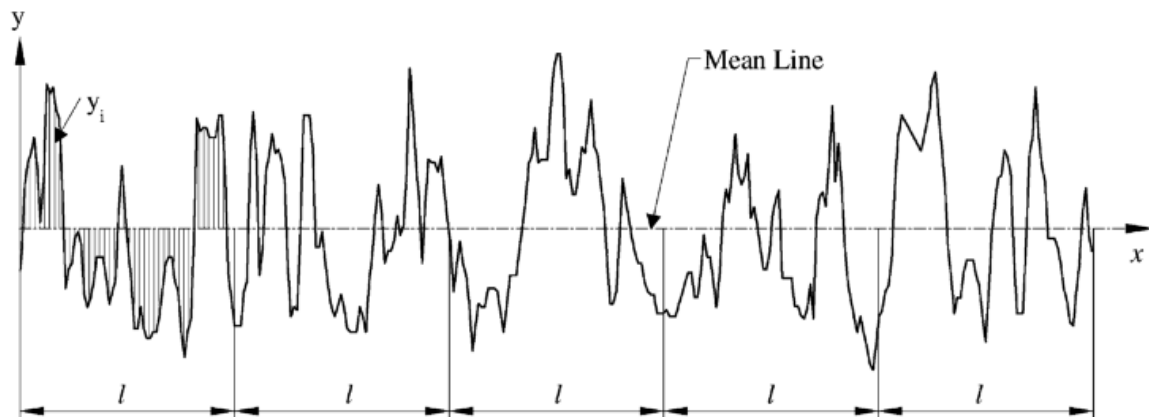


Figure 3: Arithmetic average height,  $R_a$  [12]

It important to do surface morphology and surface roughness because it can evaluate and determine the amount of filler scattering or filler agglomerate on the conductive ink, which can affect the surface roughness and then affect the current resistance inside the ink.

### 2.2.2 Bulk Resistivity

Bulk resistivity was measured by using digital multimeter at four points, which were P1, P2, P3, and P4. P1 until P3 like mentioned in Figure 2 and P4 is end-to-end of the ink. Most digital multimeter measured down to  $0.1 \Omega$  and some of it might go as high as  $300 M\Omega$ . Firstly, negative probe was placed at the start of conductive ink track and positive probe was placed on four marked points starting from P1 until P4. This test was done to measure bulk resistivity that



flowed along the ink track for each mark distance. The track or circuit must be powered off when measuring the resistivity or must be tested with the absence of voltage to avoid damages on the circuit.

From this test, changes of resistance in straight line, turn or edge for each patterns can be observed. Bulk resistivity value that was obtained from multimeter was live reading, which needed to be collected manually. All these tests were conducted with three repetitions.

### 2.2.3 Sheet Resistivity

Sheet resistivity was performed using four point probe machine due to its independent of the square and fairly low resistivity of thin film[10]. All the samples were measured on marked points as in Figure 2. Firstly, before starting the measuring process, calibration by using reference sample, an indium-tin-oxide (ITO) coated glass was done to ensure the device was functioning well and accurate. Referenced sample was put on the device base under probe pin which had four probes and the height of probe pin was lowered until it touched the referenced sample. All the four probes must be in parallel and touched the referenced sample because the current,  $I$  flows through outer probes and induces a voltage,  $V$  in the inner voltage probes as shown in Figure 4. From the set-up as in Figure 4, sheet resistivity can also be defined with mathematical equation as below;

$$\rho = 2\pi s \frac{V}{I}$$

When all the probes touched the referenced sample, they started to take live reading of the sample. Due to live measurement, RC (resistance-capacitance) delay was needed as the current inside the sample needed some time to climb up or down to reach saturation value.

To measure the experimental samples, all calibration steps were repeated on it. Before that, probe pin height needed to be adjusted again to gain suitable height for the experimental samples because PET substrate and referenced sample have different thickness. When the value was obtained, enter button was pushed to save the measured value. Lastly, the collected data was imported into its software. Moreover, all tests were conducted with three repetitions

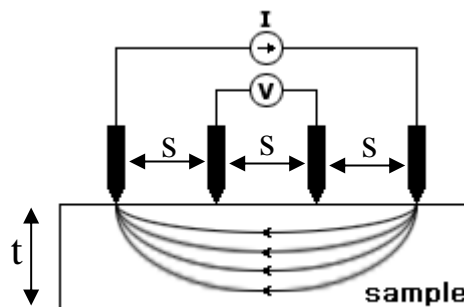


Figure 4: Four-point probe schematic set-up

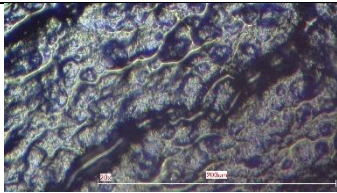
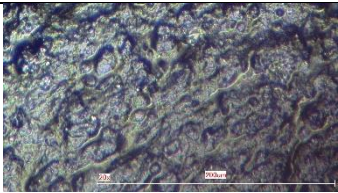
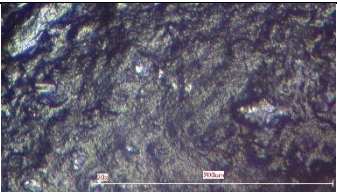
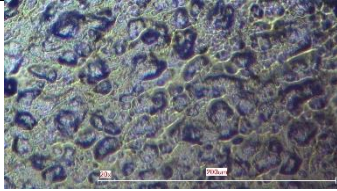
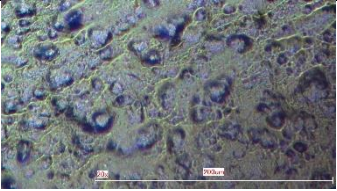
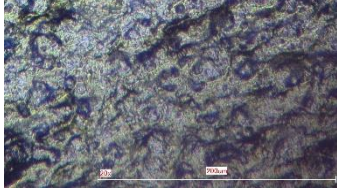
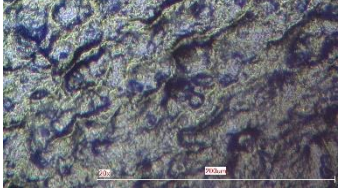
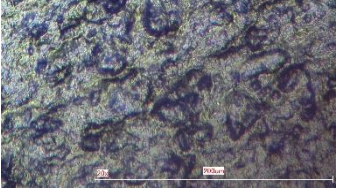
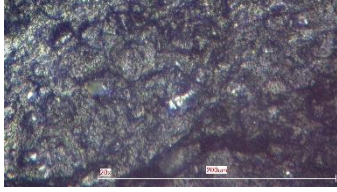
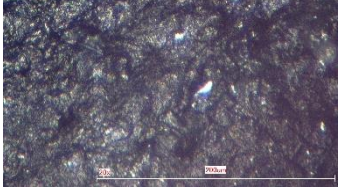
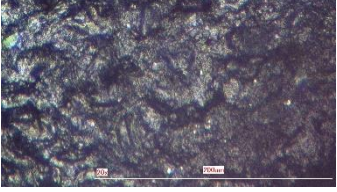
## 3. RESULTS AND DISCUSSION

### 3.1 Surface Morphology and Roughness

Table 1 shows conductive ink surface microstructure condition for each samples. From the image in table 1, granular particles with big quantity and size can be observed on surface of all sample with 1 mm track width. Granular particles occurred when there were conglomeration of discrete solid such as filler particle in one point. This phenomenon may obstruct current conductivity inside the ink. According to Kim D., & Moon J. in 2005, granular particle that had been formed needed to have 3D connection that caused the particle necking and growth into continuous connection. The granular particle can be conductive even though it was still porous. But, in this case there were formation of granular particle only with no continuous connection. This situation increased the resistance inside the ink. Furthermore, the printed ink for 1 mm width was formed with many layers, which gave resistance changes when current flow through it and also gave higher value of surface roughness.

Image microstructure for 2 mm of track width had shown there were less granular particle formed and smoother than 1 mm width. Moreover, 3 mm of track had lesser granular particle and smoothest surface roughness.

Table 1. Sample's surface morphology

Pattern	Width	Surface Morphology		
		Point 1	Point 2	Point 3
Straight	1 mm			
	2 mm			
	3 mm			
Curve	1 mm			

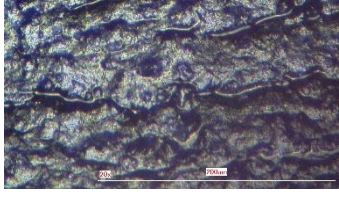
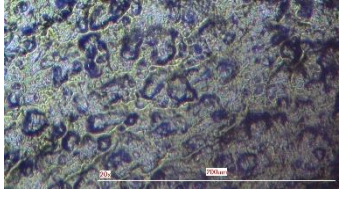
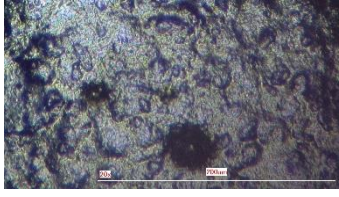
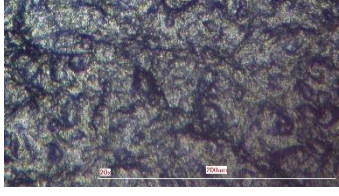
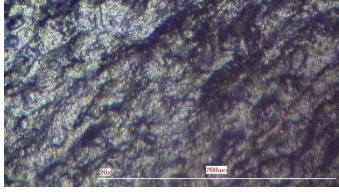
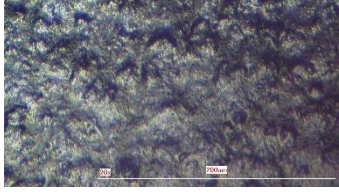
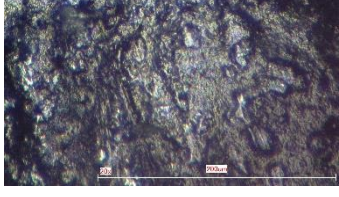
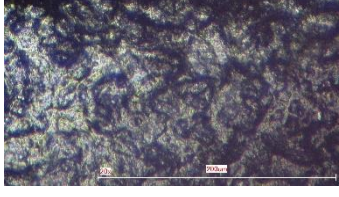
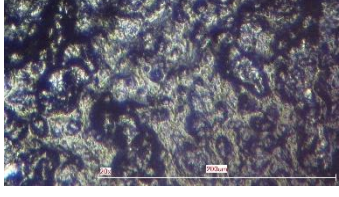
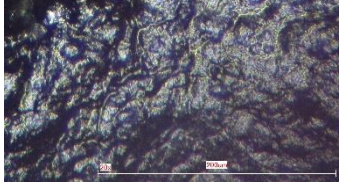
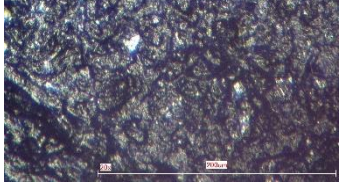
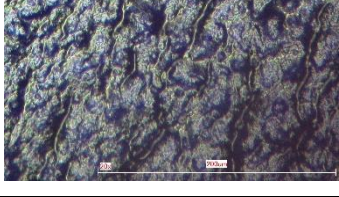
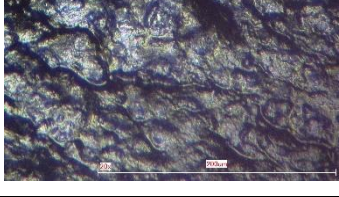
Curve	2 mm			
	3 mm			
Square	1 mm			
	2 mm			
	3 mm			
Zig-zag	1 mm			
	2 mm			
	3 mm			

Table 2. Result of surface roughness

Pattern	Width	Surface Roughness, Ra ( $\mu\text{m}$ )		
		P1	P2	P3
Straight	1 mm	0.33	0.30	0.63
	2 mm	0.33	0.57	0.30
	3 mm	0.33	0.43	0.33
Curve	1 mm	0.53	0.43	0.57
	2 mm	0.63	0.23	0.30
	3 mm	0.27	0.33	0.27
Square	1 mm	0.43	1.00	0.63
	2 mm	0.53	0.27	0.27
	3 mm	0.17	0.43	0.33
Zig-zag	1 mm	1.20	0.93	0.23
	2 mm	0.30	0.70	0.23
	3 mm	0.27	0.13	0.27

Other than surface morphology, average of surface roughness, Ra was also measured from 3D non-contact profilometer. Ra can also be defined as arithmetic average of mean line of absolute value of profile height deviations. All the obtained data was tabulated into Table 2 and represented into the graph that analyze the relationship between surface roughness and each point at every width size and types of patterns.

Figure 5 shows the surface images of four patterns with 1 mm, 2 mm, and 3 mm of width. The surface roughness of zig-zag pattern had highest surface roughness that decreased from 0.79  $\mu\text{m}$  to 0.41  $\mu\text{m}$  then dropped to the lowest of four pattern to 0.22  $\mu\text{m}$  with the increase of ink width from 1 mm to 3 mm. Square pattern had the second highest surface roughness at 1 mm, which was 0.69  $\mu\text{m}$  and dropped rapidly at 2 mm. It meant that filler had concentrated at observed point as compared to decreased value from width 2 mm to 3 mm. Meanwhile, surface roughness for curve pattern had decreased uniformly and straight pattern had lowest surface roughness and they decreased constantly with small gap between each width.

Therefore, Figure 4 shows decrement in surface roughness for all patterns with the increase of ink width. With increasing of ink's width, it gave more space for filler to disperse during printing process and avoid the filler from agglomeration at one point. Straight and curve patterns showed uniform and small changes between each width, which may due to no turn or less turn in ink track as compared to square and zig-zag patterns, which had sharp edges and turn. Surface roughness is commonly controlled by process parameter such as substrate temperature, working pressure and gas pressure[3]. In this experiment, the differences of ink track width

affected the changes of surface roughness since the other parameters were either consistent or not being considered for conductive ink.

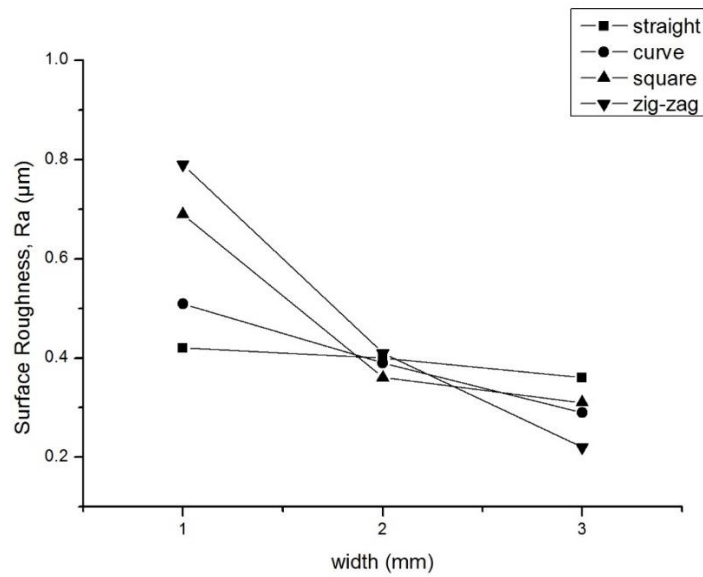


Figure 5: Surface roughness graph for 1mm, 2mm and 3mm line width for all patterns

### 3.2 Bulk Resistivity

Table 3: Data for bulk resistivity

Pattern	Width (mm)	Bulk Resistivity (kΩ)			
		P1	P2	P3	P4
Straight	1	0.341	0.579	0.981	1.240
	2	0.181	0.348	0.579	0.753
	3	0.152	0.271	0.378	0.457
Curve	1	0.283	0.677	1.360	1.591
	2	0.193	0.454	0.872	0.981
	3	0.114	0.243	0.475	0.573
Square	1	0.346	0.762	1.207	1.551
	2	0.242	0.528	0.836	1.047
	3	0.187	0.331	0.533	0.675
Zig-zag	1	0.260	0.755	1.420	1.633
	2	0.186	0.425	0.745	0.884
	3	0.110	0.298	0.524	0.615



Table 3 above shows collected data for bulk resistivity for each sample and these data then translate into of graph resistivity over distance point for each width size and pattern as in Figure 6. Figure 6 shows the bulk resistivity over point on the track, begins at P1 (2 mm), P2 (4.5 mm), P3 (7 mm), and P4 (9 mm) for four patterns like straight pattern (a), curve pattern (b), square pattern (c), and zig-zag pattern (d). In all four graphs show bulk resistivity for 1 mm width had highest resistance followed with 2 mm and 3 mm had the lowest resistance that flowed through the track. It proved that bulk resistance decreased with the increase of track width size. With bigger track width size, the more space was available inside the track to make the filler to disperse effectively, then eased the current flow and lowered the resistance existence inside the track. Other than that, all four graphs show that bulk resistivity increased with longer distance of electricity flow

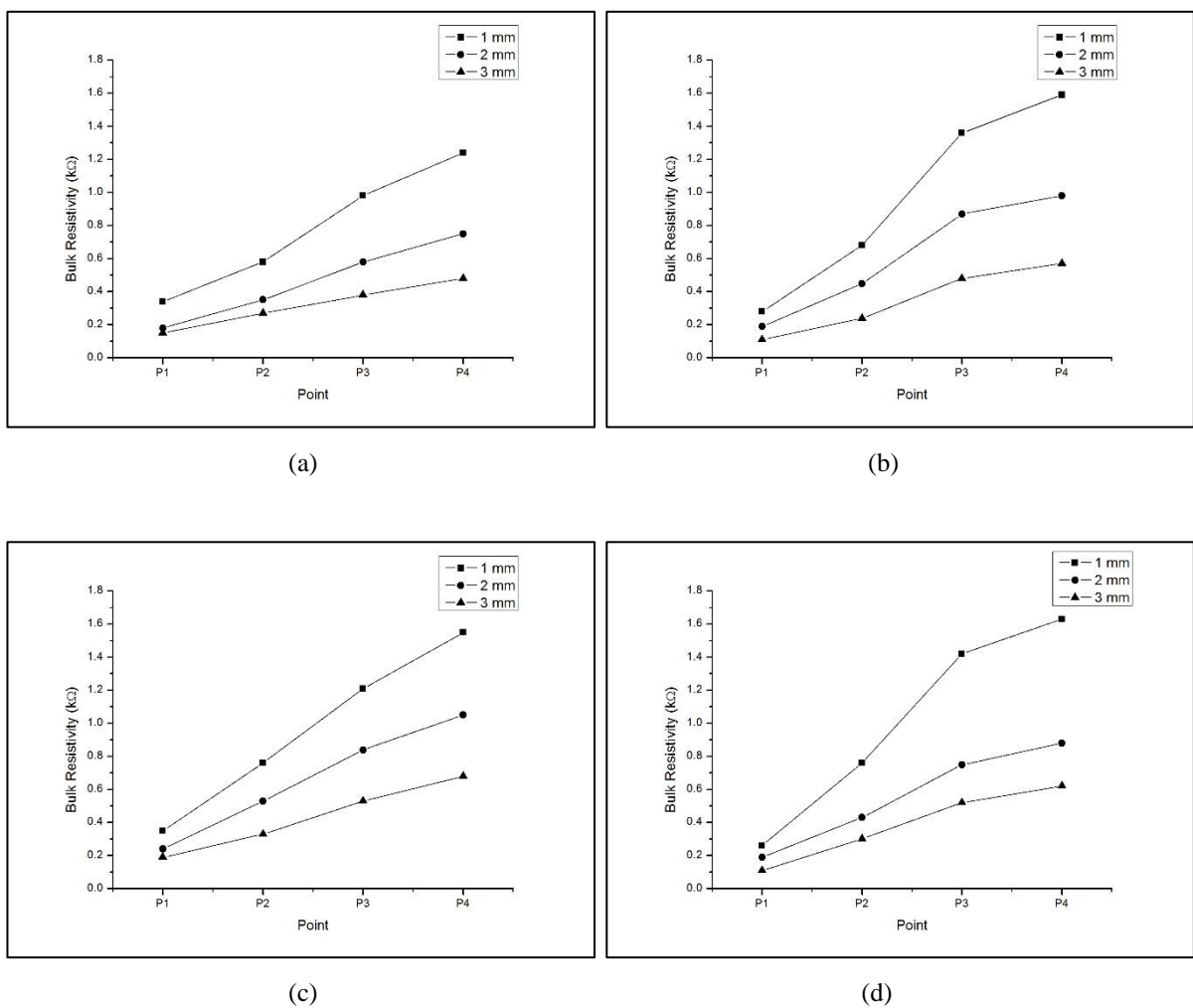


Figure 6: Graph of bulk resistivity with straight pattern (a), curve pattern (b), square pattern(c), and zig-zag pattern (d) for 1 mm, 2 mm, and 3 mm of track width.

Meanwhile, Figure 7 shows the graphs of bulk resistivity over point distance for all four patterns at 1 mm track width (a), 2 mm (b), and 3 mm (c). For graph 7(a), straight pattern had the lowest bulk resistance over point distance followed with square pattern, then curve pattern and zig-zag pattern had the highest bulk resistance. Also, the graph shows that curve and zig-zag

patterns show the lowest bulk resistance, 0.346 kΩ and 0.260 kΩ at the beginning but rise to the highest bulk resistance at P3, 1.207 kΩ and 1.420 kΩ and P4, 1.551 kΩ and 1.633 kΩ. For graph 7(b), straight pattern had the lowest bulk resistance over point distance followed with zig-zag pattern, then curve pattern and square pattern had the highest bulk resistance. All points had constant increment of bulk resistivity except for curve pattern's bulk resistivity at point P3, which increased sharply with the value of 0.872 kΩ. It exceeded the other three data at P3. Lastly, graph 7(c) shows that curve pattern had the lowest resistance at the beginning, then zig-zag, straight, and square patterns. But, curve, zig-zag, and square patterns had sharp rise with square pattern as the highest. Meanwhile, straight pattern had increment of resistance consistently with small difference gap.

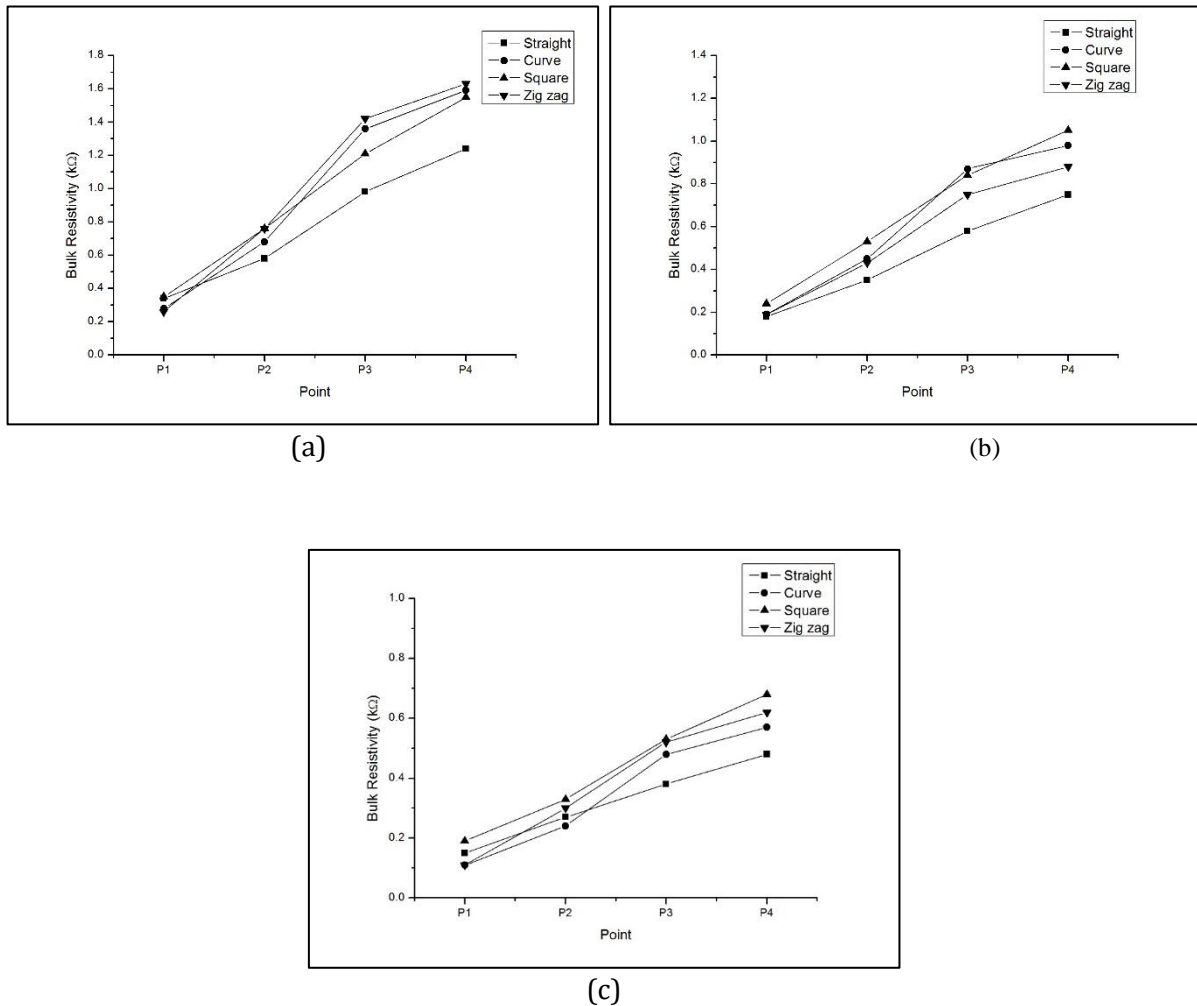


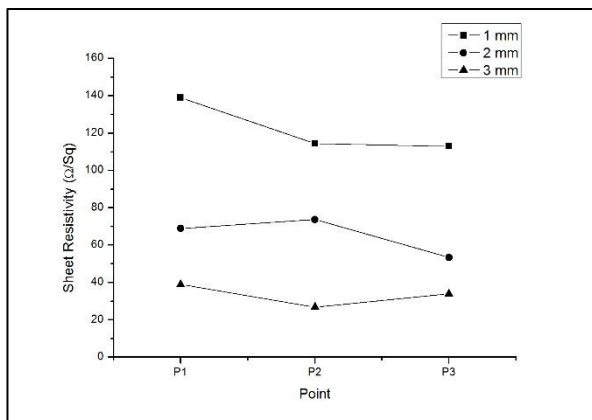
Figure 7: Graph of bulk resistivity with 1 mm track width (a), 2 mm track width (b), and 3 mm track width(c) for all four patterns.

### 3.3 Sheet Resistivity

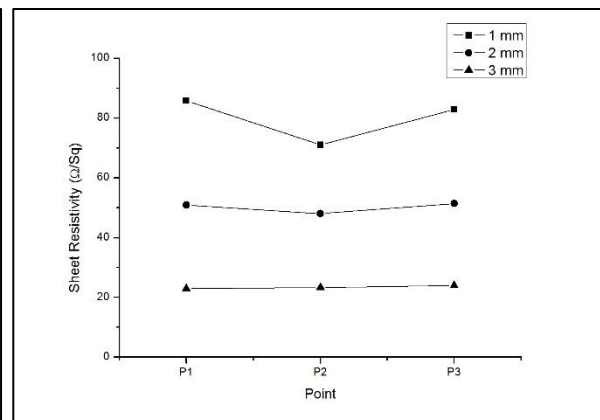
Table 4: Data for sheet resistivity

Pattern	Width (mm)	Sheet Resistivity ( $\Omega/\text{sq}$ )
Straight	1	122.10
	2	65.34
	3	33.13
Curve	1	79.94
	2	50.12
	3	23.40
Square	1	72.91
	2	38.90
	3	25.49
Zig-zag	1	105.94
	2	48.05
	3	26.90

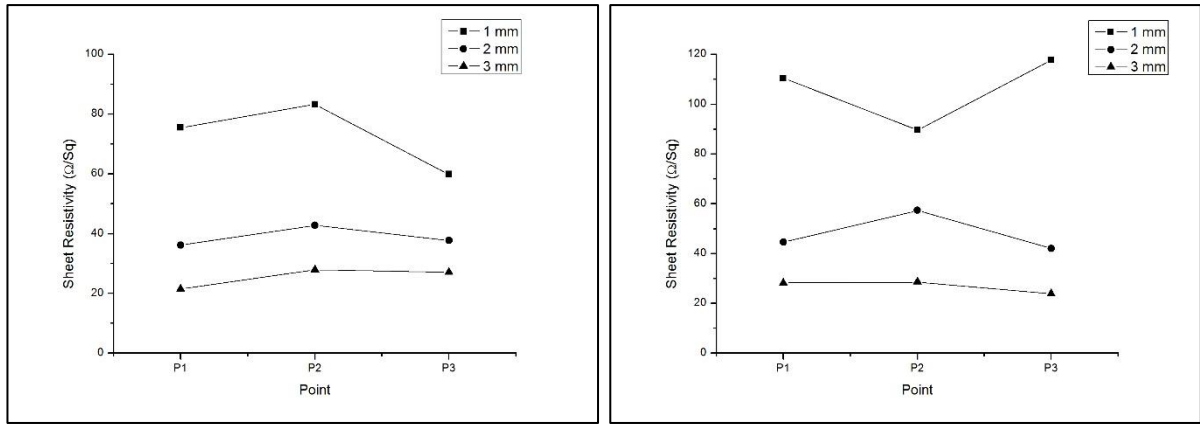
Sheet resistivity was measured with four point probe and the data was tabulated into table, then represented into graph of each pattern's sheet resistivity over point for every track width and graph of sheet resistivity over track width. Figure 8 shows sheet resistivity over point at every track width. It shows that track width of 1 mm had the highest sheet resistance, followed by 2 mm and then 3 mm width with lowest sheet resistance for all four patterns. Other than that, Figure 8 shows that track with 1 mm width had unstable and sharp increase or decrease of resistance values as compared to track with 2 mm and 3 mm width, which were more stable and had value increment with small differences. In these cases, sheet resistivity was highest with small track width and decreased as the width increased due to filler particle that had dispersed excellently. When the width became small or narrow, the filler particles were tended to agglomerate together and hindered the electrical conductivity.



(a)



(b)



(c) (d)

Figure 8: Graph of sheet resistivity with straight pattern (a), curve pattern (b), square pattern(c), and zig-zag pattern (d) for 1 mm, 2 mm, and 3 mm of track width.

Results of sheet resistivity over track width for every patterns were shown in Figure 9. Square pattern had the lowest sheet resistivity with the increase of the track width. Then, it followed with curve, and zig-zag patterns. Straight pattern showed the highest sheet resistivity for all four patterns

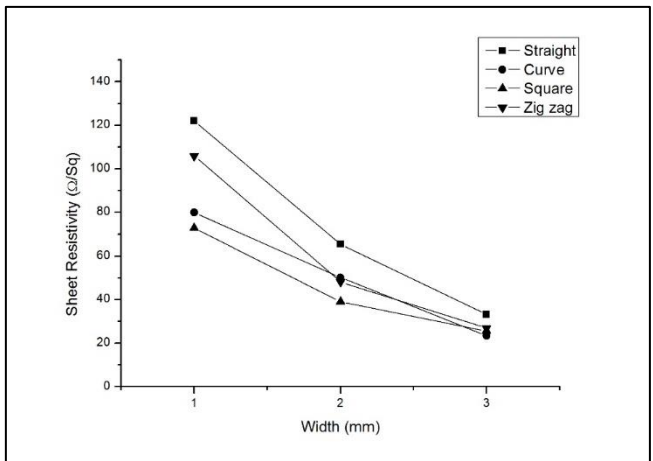


Figure 9: Graph of sheet resistivity over track width for all four patterns

#### 4. CONCLUSION

Stencil printing method was used to make the liquid-solid conductive ink on PET as substrate. Results was obtained with different parameters such as track width, and track pattern. Furthermore, the samples were prepared and measured under unloaded condition. From observation with profilometer, granular particles were formed less and far apart when the track width increased. Surface roughness of the ink also became smoother when track width was increased and straight pattern had small decrement and changes at three points as compared to zig-zag pattern, which surface roughness decreased sharply at three points.

There were also sheet resistivity and bulk resistivity that were measured with four point probe and multimeter. These two results had the same outcome, which the resistivity decreased with the increment of track width. Zig-zag pattern had higher sheet resistivity and straight pattern had lowest sheet resistivity. Meanwhile, for all three track width, straight pattern had lowest bulk resistivity and zig-zag pattern had highest bulk resistivity for 1 mm track width. Meanwhile, square pattern had the highest bulk resistivity for 2 mm and 3 mm track width. From all the obtained results, straight pattern showed the best result as compared to other patterns. This was because other pattern had edge and sharp corner, which hindered the electrical conductivity and increased their resistivity.

#### REFERENCES

- [1] Z. Wang, W. Wang, Z. Jiang, and D. Yu, "Low temperature sintering nano-silver conductive ink printed on cotton fabric as printed electronics," *Prog. Org. Coatings*, vol. 101, pp. 604–611, 2016.
- [2] J. Kastner, T. Faury, H. M. Außerhuber, T. Obermüller, H. Leichtfried, M. J. Haslinger, E. Liftinger, J. Innerlohinger, I. Gnatiuk, D. Holzinger, and T. Lederer, "Silver-based reactive ink for inkjet-printing of conductive lines on textiles," *Microelectron. Eng.*, vol. 176, pp. 84–88, 2017.
- [3] W. Tang, Y. Chao, X. Weng, L. Deng, and K. Xu, "Optical Property and the Relationship between Resistivity and Surface Roughness of Indium Tin Oxide Thin Films," vol. 32, pp. 680–686, 2012.
- [4] S. Son, Y. Cho, J. Rha, and C. Choi, "Fabrication of metal electrodes on flexible substrates by controlled deposition of conductive nano-ink," *Mater. Lett.*, vol. 117, pp. 179–183, 2014.
- [5] E. Britannica, "Polyethylene Terephthalate." Encyclopaedia Britannica, inc, pp. 1–3, 2019.
- [6] T. S. Tran, N. K. Dutta, and N. R. Choudhury, "Graphene inks for printed flexible electronics: graphene dispersions, ink formulations, printing techniques and applications," *Adv. Colloid Interface Sci.*, p. #pagerange#, 2018.
- [7] H. Mekar, "Thermal and ultrasonic bonding between planar polyethylene terephthalate , acrylonitrile butadiene styrene , and polycarbonate substrates," *Int. J. Adhes. Adhes.*, vol. 84, no. April, pp. 394–405, 2018.
- [8] S. H. Kim, T. Min, J. W. Choi, S. H. Baek, J. Choi, and C. Aranas, "Ternary Bi<sub>2</sub>Te<sub>3</sub>–In<sub>2</sub>Te<sub>3</sub>–Ga<sub>2</sub>Te<sub>3</sub> (n-type) thermoelectric film on a flexible PET substrate for use in wearables Sang," *Energy*, vol. 3, 2018.
- [9] B. Marinho, M. Ghislandi, E. Tkalya, C. E. Koning, and G. De With, "Electrical conductivity of compacts of graphene , multi-wall carbon nanotubes , carbon black , and graphite powder," *Powder Technol.*, vol. 221, pp. 351–358, 2012.
- [10] S. Merilampi and P. Ruuskanen, "The characterization of electrically conductive silver ink patterns on flexible substrates," *Microelectron. Reliab.*, vol. 49, no. 7, pp. 782–790, 2009.
- [11] J. Wei, T. Vo, and F. Inam, "Epoxy/graphene nanocomposites – processing and properties: a review," *RSC Adv.*, vol. 5, pp. 73510–73524, 2015.
- [12] T. M. A. Maksoud, I. M. Elewa, H. Soliman, and P. Media, "Roughness parameters," vol. 8, no. 2, pp. 263–276, 2016.